

# <sup>1</sup> COSMOS: A numerical relativity code specialized for PBH formation

<sup>3</sup> **Chul-Moon Yoo**  <sup>1,2</sup>, **Hirotada Okawa**  <sup>3</sup>, **Albert Escrivà**  <sup>1</sup>, **Tomohiro Harada**  <sup>4</sup>, **Hayami Iizuka**  <sup>4</sup>, **Taishi Ikeda**  <sup>5</sup>, **Yasutaka Koga**  <sup>6</sup>, **Daiki Saito**  <sup>7</sup>, **Masaaki Shimada**  <sup>1</sup>, and **Koichiro Uehara**  <sup>1</sup>

<sup>6</sup> 1 Graduate School of Science, Nagoya University, Japan 2 Kobayashi Maskawa Institute, Nagoya University, Japan 3 Faculty of Software and Information Technology, Aomori University, Japan 4 Department of Physics, Rikkyo University, Japan 5 Center of Gravity, Niels Bohr Institute, Denmark 6 Department of Information and Computer Science, Osaka Institute of Technology, Japan 7 Department of Physics, Kyoto University, Japan

DOI: [10.xxxxxx/draft](https://doi.org/10.xxxxxx/draft)

## Software

- [Review](#) 
- [Repository](#) 
- [Archive](#) 

Editor: [Fruzsina Agocs](#)  

## Reviewers:

- [@ShaunFell](#)

Submitted: 16 February 2025

Published: unpublished

## License

Authors of papers retain copyright and release the work under a Creative Commons Attribution 4.0 International License ([CC BY 4.0](#)).<sup>23</sup>

## <sup>11</sup> Summary

<sup>12</sup> Primordial black holes (PBHs) are black holes generated in the early universe without experience of the form of a star. It has been pointed out that PBHs may be candidates for black holes and compact objects of various masses in the universe or a major component of dark matter. In particular, PBHs have been attracting much attention in the recent development of gravitational wave observation. In the standard formation process, PBHs are formed from super-horizon primordial fluctuations with non-linearly large initial amplitude. In order to follow the whole non-linear gravitational dynamics, one has to rely on numerical relativity solving Einstein equations. COSMOS ([Okawa et al., 2014; Yoo et al., 2013](#)) provides simple tools for the simulation of PBH formation (see COSMOS-S <sup>1</sup> for a spherically symmetric version of COSMOS). COSMOS is a C++ packages for solving Einstein equations in 3+1 dimensions. It was originally translated from SACRA code ([Yamamoto et al., 2008](#)) into C++ and has been developed specialized for PBH formation. In this paper, we do not describe all scientific results obtained by using COSMOS. The readers who are interested in the past achievements may refer to Yoo et al. (2013); Okawa et al. (2014); Yoo & Okawa (2014); Okawa & Cardoso (2014); Ikeda et al. (2015); Brito et al. (2015); Brito et al. (2016); Okawa (2015); Yoo et al. (2017); Yoo et al. (2019); Yoo (2024); Escrivà & Yoo (2024b); Escrivà & Yoo (2024a); <sup>2</sup>.

## <sup>28</sup> Statement of need

<sup>29</sup> In the simulation of PBH formation, since there is a hierarchy between the size of the collapsing region and cosmological expansion scale, an efficient resolution refinement procedure is needed. <sup>30</sup> In order to resolve the collapsing region, non-Cartesian scale-up coordinates ([Yoo et al., 2019](#)) <sup>31</sup> and a fixed mesh-refinement procedure ([Yoo, 2024](#)) are implemented in COSMOS. To achieve a <sup>32</sup> practically acceptable computational speed, an OpenMP package is used for the parallelization. <sup>33</sup> No other packages are required, and the functionality is minimal. Therefore it would be easy to <sup>34</sup> use for beginners of numerical relativity. A perfect fluid with a linear equation of states and a <sup>35</sup> massless scalar field are implemented as matter fields. Once users understand the source code <sup>36</sup> to some extent, the system can be easily extended to various scientifically interesting settings. <sup>37</sup>

<sup>1</sup><https://github.com/cmyoo/cosmos-s> .

<sup>2</sup>In most of the references: Yoo et al. (2013); Okawa et al. (2014); Yoo & Okawa (2014); Okawa & Cardoso (2014); Ikeda et al. (2015); Brito et al. (2015); Brito et al. (2016); Okawa (2015); Yoo et al. (2017); Yoo et al. (2019); Yoo (2024); Escrivà & Yoo (2024b); Escrivà & Yoo (2024a), additional functions and packages have been implemented to meet the requirements for individual settings. Therefore the results may not be obtained by simply running the public code.

## <sup>38</sup> Physical system settings

<sup>39</sup> Einstein equations

$$G_{\mu\nu} = R_{\mu\nu} - \frac{1}{2}Rg_{\mu\nu} = \frac{8\pi G}{c^4}T_{\mu\nu}$$

<sup>40</sup> are solved, where  $G_{\mu\nu}$ ,  $g_{\mu\nu}$ ,  $R_{\mu\nu}$ ,  $R$ ,  $G$ ,  $c$  and  $T_{\mu\nu}$  are the Einstein tensor, metric tensor, Ricci tensor, Ricci scalar, Newtonian gravitational constant, speed of light and energy momentum tensor, respectively. The energy momentum tensor is divided into the fluid and scalar field contributions as follows:

$$T_{\mu\nu} = T_{\mu\nu}^{\text{SC}} + T_{\mu\nu}^{\text{FL}}$$

<sup>44</sup> with

$$T_{\mu\nu}^{\text{SC}} = \nabla_\mu \phi \nabla_\nu \phi - \frac{1}{2}g_{\mu\nu} \nabla^\lambda \phi \nabla_\lambda \phi$$

<sup>45</sup> and

$$T_{\mu\nu}^{\text{FL}} = (\rho + P)u_\mu u_\nu + Pg_{\mu\nu},$$

<sup>46</sup> where  $\nabla$ ,  $\phi$ ,  $\rho$ ,  $u_\mu$  and  $P$  are the covariant derivative associated with  $g_{\mu\nu}$ , scalar field, fluid <sup>47</sup> energy density, four-velocity and pressure, respectively. The pressure and the energy density <sup>48</sup> are assumed to satisfy the linear equation of state  $P = w\rho$  with  $w$  being a constant. The <sup>49</sup> equations of motion for the scalar field

$$\nabla^\mu \nabla_\mu \phi = 0$$

<sup>50</sup> and the fluid

$$\nabla^\mu T_{\mu\nu}^{\text{FL}} = 0$$

<sup>51</sup> are also solved. Readers are asked to refer to standard textbooks of numerical relativity (e.g., <sup>52</sup> Gourgoulhon (2012); Shibata (2016)) to learn how to rewrite these equations into a form <sup>53</sup> suitable for numerical integration. To solve the fluid equations of motion, we basically follow <sup>54</sup> the scheme discussed in Kurganov & Tadmor (2000); Shibata & Font (2005).

<sup>55</sup> As for the initial data, we adopt the long-wavelength growing-mode solutions up through <sup>56</sup> the next-leading order of the expansion parameter  $\epsilon = k/(aH) \ll 1$ , where  $1/k$  gives the <sup>57</sup> characteristic comoving scale of the inhomogeneity, and  $a$  and  $H$  are the scale factor and Hubble <sup>58</sup> expansion rate in the reference background universe. The initial data can be characterized <sup>59</sup> by a function of the spatial coordinates  $\vec{x}$  as the curvature perturbation  $\zeta(\vec{x})$  for adiabatic <sup>60</sup> fluctuations (Harada et al., 2015; Yoo et al., 2020; Yoo, 2024) and iso-curvature perturbation <sup>61</sup>  $\Upsilon(\vec{x})$  for massless scalar iso-curvature (Yoo et al., 2022). Since the space is filled with the <sup>62</sup> fluid, the initial fluid distribution can be generated to meet the constraint equations included <sup>63</sup> in the Einstein equations. Then, the constraint equations are initially satisfied within the <sup>64</sup> machine's precision. Therefore, the constraint equations are not solved by integrating elliptic <sup>65</sup> differential equations. This is very different from the standard method to obtain the initial <sup>66</sup> data for spacetimes with asymptotically flat vacuum regions. This is why elliptic solvers for <sup>67</sup> constraint equations are not included in this package.

## <sup>68</sup> Examples

<sup>69</sup> Three examples are included in the package. These examples are intended primarily for <sup>70</sup> demonstration and instructional purposes, and thus, the precision is not a primary concern. <sup>71</sup> The resolution has been intentionally kept to a minimum. In the figures below, the length <sup>72</sup> scale is normalized by the size  $L$  of the box for the numerical simulation.

<sup>73</sup> **Evolution of a single-mode perturbation**

<sup>74</sup> The evolution of sinusoidal small fluctuation is given as an example, which can be compared  
<sup>75</sup> with the corresponding linear perturbation (see Figure 1).

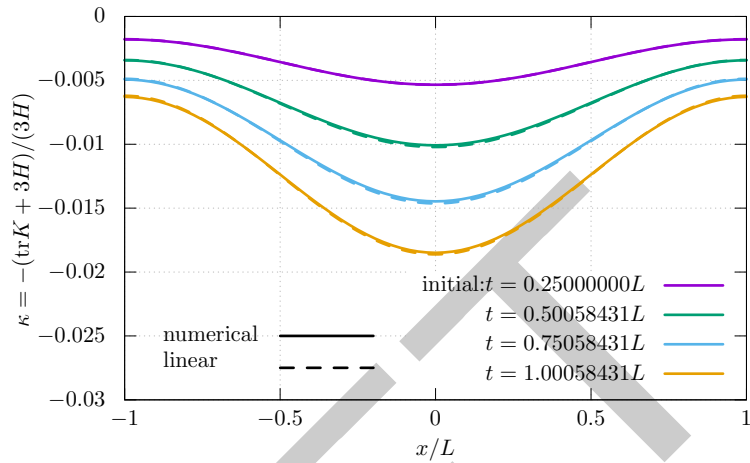


**Figure 1:** The time evolution of the trace of the extrinsic curvature  $\text{tr}K$  is compared with the solution of the linear perturbation equation.

<sup>76</sup> **Adiabatic spherically symmetric initial fluctuation**

<sup>77</sup> The scalar field is absent in this example. The setting is similar to that in Yoo et al. (2020).  
<sup>78</sup> We also attach the data obtained by solving the Einstein equations until an apparent horizon  
<sup>79</sup> is found (see Figure 2 and Figure 3).

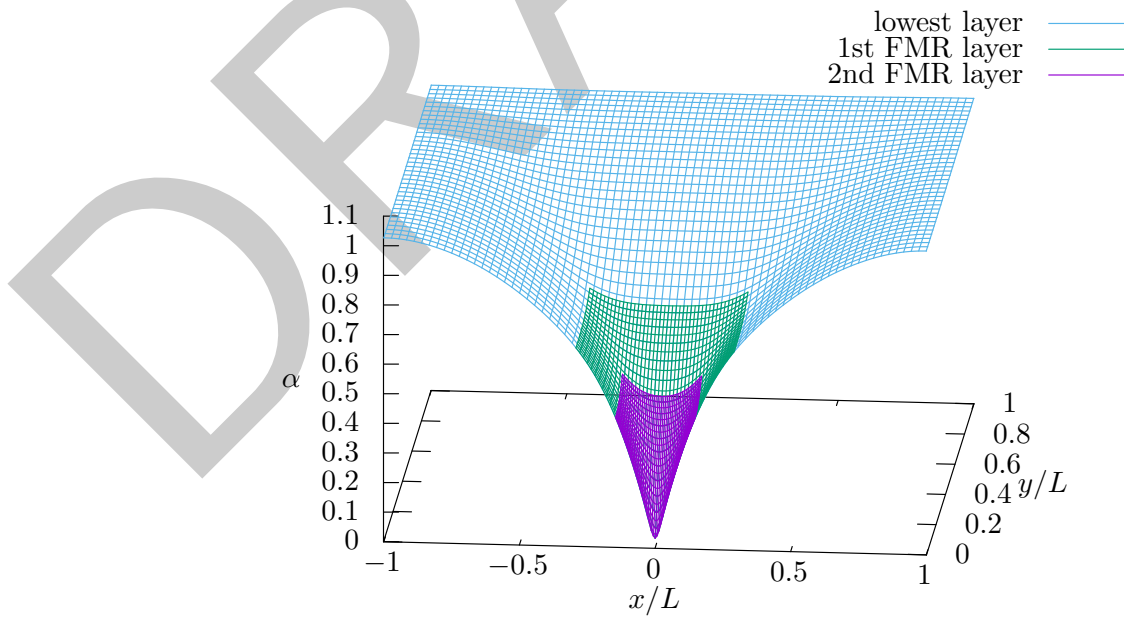


**Figure 2:** The lapse function (“ $tt$ -component” of the metric) on the  $xy$ -plane at the time when an apparent horizon is found.

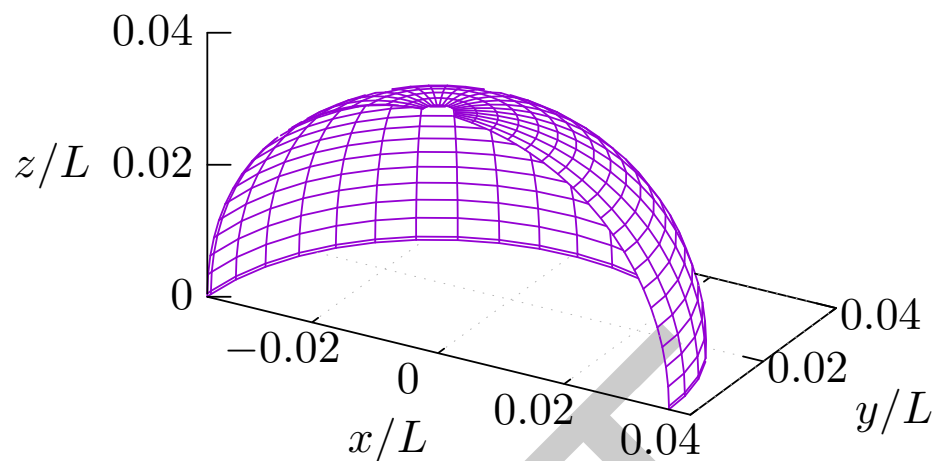


**Figure 3:** The shape of the apparent horizon when it is found.

**80 Spherically symmetric iso-curvature**

**81** The setting is similar to that in Yoo et al. (2022). We also attach the data obtained by solving  
**82** the Einstein equations until an apparent horizon is found.

**83 Acknowledgements**

**84** A.E. acknowledges support from the JSPS Postdoctoral Fellowships for Research in Japan  
**85** (Graduate School of Sciences, Nagoya University). K.U. would like to take this opportunity  
**86** to thank the “THERS Make New Standards Program for the Next Generation Researchers”  
**87** supported by JST SPRING, Grant Number JPMJSP2125. T.I. acknowledges support from  
**88** VILLUM Foundation (grant no. VIL37766) and the DNRF Chair program (grant no. DNRF162)  
**89** by the Danish National Research Foundation. This work is supported in part by JSPS KAKENHI  
**90** Grant Nos. 20H05850 (C.Y.), 20H05853 (T.H., C.Y.), 21K20367 (Y.K.), 23KK0048 (Y.K.),  
**91** 24K07027 (T.H., C.Y.), 24KJ1223 (D.S.), and 25K07281 (C.Y.).

**92 References**

- 93** Brito, R., Cardoso, V., Macedo, C. F. B., Okawa, H., & Palenzuela, C. (2016). Interaction  
**94** between bosonic dark matter and stars. *Phys. Rev. D*, 93(4), 044045. <https://doi.org/10.1103/PhysRevD.93.044045>
- 96** Brito, R., Cardoso, V., & Okawa, H. (2015). Accretion of dark matter by stars. *Phys. Rev. Lett.*, 115(11), 111301. <https://doi.org/10.1103/PhysRevLett.115.111301>
- 98** Escrivà, A., & Yoo, C.-M. (2024a). *Non-spherical effects on the mass function of Primordial  
**99** Black Holes*. <https://arxiv.org/abs/2410.03451>
- 100** Escrivà, A., & Yoo, C.-M. (2024b). *Simulations of Ellipsoidal Primordial Black Hole Formation*.  
**101** <https://arxiv.org/abs/2410.03452>
- 102** Gourgoulhon, E. (2012). *3+1 formalism in general relativity : Bases of numerical relativity*.  
**103** Springer. <https://doi.org/10.1007/978-3-642-24525-1>
- 104** Harada, T., Yoo, C.-M., Nakama, T., & Koga, Y. (2015). Cosmological long-wavelength  
**105** solutions and primordial black hole formation. *Phys. Rev. D* 91(8), 084057. <https://doi.org/10.1103/PhysRevD.91.084057>
- 107** Ikeda, T., Yoo, C.-M., & Nambu, Y. (2015). Expanding universe with nonlinear gravitational

- 108 waves. *Phys. Rev. D*, 92(4), 044041. <https://doi.org/10.1103/PhysRevD.92.044041>
- 109 Kurganov, A., & Tadmor, E. (2000). New High-Resolution Central Schemes for Nonlinear  
110 Conservation Laws and Convection-Diffusion Equations. *J. Comput. Phys.*, 160, 241–282.  
111 <https://doi.org/10.1006/jcph.2000.6459>
- 112 Okawa, H. (2015). Nonlinear evolutions of bosonic clouds around black holes. *Classical and  
113 Quantum Gravity*, 32(21), 214003. <https://doi.org/10.1088/0264-9381/32/21/214003>
- 114 Okawa, H., & Cardoso, V. (2014). Black holes and fundamental fields: Hair, kicks, and a  
115 gravitational Magnus effect. *Phys. Rev. D*, 90(10), 104040. <https://doi.org/10.1103/PhysRevD.90.104040>
- 117 Okawa, H., Witek, H., & Cardoso, V. (2014). Black holes and fundamental fields in Numerical  
118 Relativity: initial data construction and evolution of bound states. *Phys. Rev. D*, 89(10),  
119 104032. <https://doi.org/10.1103/PhysRevD.89.104032>
- 120 Shibata, M. (2016). *Numerical relativity*. World Scientific Publishing Co. Pte. Ltd. <https://doi.org/10.1142/9692>
- 122 Shibata, M., & Font, J. A. (2005). Robustness of a high-resolution central scheme for  
123 hydrodynamic simulations in full general relativity. *Phys. Rev. D*, 72, 047501. <https://doi.org/10.1103/PhysRevD.72.047501>
- 125 Yamamoto, T., Shibata, M., & Taniguchi, K. (2008). Simulating coalescing compact binaries  
126 by a new code SACRA. *Phys. Rev. D*, 78, 064054. <https://doi.org/10.1103/PhysRevD.78.064054>
- 128 Yoo, C.-M. (2024). Primordial black hole formation from a nonspherical density profile with a  
129 misaligned deformation tensor. *Phys. Rev. D*, 110(4), 043526. <https://doi.org/10.1103/PhysRevD.110.043526>
- 131 Yoo, C.-M., Harada, T., Hirano, S., Okawa, H., & Sasaki, M. (2022). Primordial black  
132 hole formation from massless scalar isocurvature. *Phys. Rev. D*, 105(10), 103538.  
133 <https://doi.org/10.1103/PhysRevD.105.103538>
- 134 Yoo, C.-M., Harada, T., & Okawa, H. (2017). 3D Simulation of Spindle Gravitational  
135 Collapse of a Collisionless Particle System. *Class. Quant. Grav.*, 34(10), 105010. <https://doi.org/10.1088/1361-6382/aa6ad5>
- 137 Yoo, C.-M., Harada, T., & Okawa, H. (2020). Threshold of Primordial Black Hole Formation  
138 in Nonspherical Collapse. *Phys. Rev. D*, 102(4), 043526. <https://doi.org/10.1103/PhysRevD.102.043526>
- 140 Yoo, C.-M., Ikeda, T., & Okawa, H. (2019). Gravitational Collapse of a Massless Scalar  
141 Field in a Periodic Box. *Class. Quant. Grav.*, 36(7), 075004. <https://doi.org/10.1088/1361-6382/ab06e2>
- 143 Yoo, C.-M., & Okawa, H. (2014). Black hole universe with a cosmological constant. *Phys.  
144 Rev. D*, 89(12), 123502. <https://doi.org/10.1103/PhysRevD.89.123502>
- 145 Yoo, C.-M., Okawa, H., & Nakao, K. (2013). Black Hole Universe: Time Evolution. *Phys.  
146 Rev. Lett.*, 111, 161102. <https://doi.org/10.1103/PhysRevLett.111.161102>